Abdominal Radiology
https://doi.org/10.1007/s00261-019-02299-3

REVIEW

# State-of-the-art in radiomics of hepatocellular carcinoma: a review of basic principles, applications, and limitations

**Joao Manoel Miranda Magalhaes Santos[1] · Brunna Clemente Oliveira[2,3] · Jose de Arimateia Batista Araujo-Filho[2] · Antonildes N. Assuncao-Jr[4] · Felipe Augusto de M. Machado[5] · Camila Carlos Tavares Rocha[1] · Joao Vicente Horvat[1,2] · Marcos Roberto Menezes[1,2] · Natally Horvat[1,2]**



## Abstract

Radiomics is a new field in medical imaging with the potential of changing medical practice. Radiomics is characterized by the extraction of several quantitative imaging features which are not visible to the naked eye from conventional imaging modalities, and its correlation with specific relevant clinical endpoints, such as pathology, therapeutic response, and survival. Several studies have evaluated the use of radiomics in patients with hepatocellular carcinoma (HCC) with encouraging results, particularly in the pretreatment prediction of tumor biological characteristics, risk of recurrence, and survival. In spite of this, there are limitations and challenges to be overcome before the implementation of radiomics into clinical routine. In this article, we will review the concepts of radiomics and their current potential applications in patients with HCC. It is important that the multidisciplinary team involved in the treatment of patients with HCC be aware of the basic principles, benefits, and limitations of radiomics in order to achieve a balanced interpretation of the results toward a personalized medicine.

**Keywords** Hepatocellular carcinoma · Radiomics · Textural analysis · Liver neoplasms · Magnetic resonance imaging · Computed tomography · Positron emission tomography

## Introduction

Hepatocellular carcinoma (HCC) is the most common primary cancer of the liver, the second leading cause of cancer mortality worldwide and the primary cause of death in patients with cirrhosis [1, 2]. The prognosis of HCC strongly depends on its stage at the time of diagnosis [3], since patients with advanced stage HCC at time of diagnosis have a poor prognosis [3–5].

✉ Natally Horvat
natallymhorvat@gmail.com

Joao Manoel Miranda Magalhaes Santos
joaomirandassa@gmail.com

Brunna Clemente Oliveira
deoliveira.brunna@gmail.com

Jose de Arimateia Batista Araujo-Filho
ariaraujocg@gmail.com

Antonildes N. Assuncao-Jr
antonildes@gmail.com

Felipe Augusto de M. Machado
felipe.augusto.machado@usp.br

Camila Carlos Tavares Rocha
camilatavarees@gmail.com

Joao Vicente Horvat
joaohorvat@gmail.com

Marcos Roberto Menezes
menezesmr@gmail.com

1 Department of Radiology, University of São Paulo, São Paulo, Brazil

2 Department of Radiology, Hospital Sírio-Libanês, Adma Jafet, 91, Bela Vista, São Paulo, SP 01308-050, Brazil

3 Department of Radiology, Hospital Samaritano, São Paulo, Brazil

4 Research and Education Institute, Hospital Sírio-Libanês, São Paulo, Brazil

5 Polytechnic School, University of São Paulo, São Paulo, Brazil

Published online: 09 November 2019

Imaging plays a critical role in the screening, early detection and management of patients with HCC [6, 7]. Up to now, imaging assessment of HCC is based on evaluation of tumor size and subjective interpretation of qualitative imaging descriptors, which are prone to variability [8]. But recent advances, especially in radiomics, have provided new tools that can potentially address this variability and provide information not previously available.

Radiomics is an emerging field that converts medical imaging into high-dimensional mineable features, providing a quantitative assessment of the image [9]. These features can then be associated to clinical endpoints, such as pathology, therapeutic response, and survival [10]. With the quantitative analysis of digital imaging, radiomics can potentially detect specific characteristics of a disease that otherwise could not be accessed visually with a potential to inform future precision medicine [9].

In the past decade, several studies have investigated radiomics in patients with HCC using computed tomography (CT) and magnetic resonance imaging (MRI) [11–30] to personalize clinical decisions and improve individualized treatment selection. These studies primarily assessed radiomics to develop diagnostic models and potential imaging biomarkers of treatment response and prognosis, such as noninvasive prediction of microvascular invasion (MVI), overall survival, recurrence, and treatment response.

Despite these encouraging results, there are limitations and challenges to be overcome before the implementation of radiomics into routine clinical practice, particularly related to heterogeneous study population, limited sample size, model design, and lack of robust validation sets. Thus, clinical investigators and radiologists should be aware of the basic principles, applications and limitations of radiomics to critically assess the clinical potential and implementation.

The purpose of this article is to explore the concepts and limitations underlying radiomics and review recent studies and potential applications in HCC texture analyses.

## Radiomics

### Definition

Radiomics is characterized by the extraction of quantitative imaging features from conventional imaging modalities using computer based algorithms and the correlation of these features with relevant clinical endpoints, such as pathology, therapeutic response, and survival [9]. These quantitative data are called radiomics features, of which texture features are a subset.

### Radiomics step-by-step process

The radiomics pipeline includes the following steps (Fig. 1):

(1) Image acquisition;
(2) Dataset creation according to the aim of the study;
(3) Exportation of the DICOM (Digital Imaging and Communications in Medicine) images from PACS (Picture Archiving and Communication System) to a workstation with computer software that will be used to perform image segmentation;
(4) Image segmentation using a single tumor area [region of interest (ROI)], or the entire tumor volume [volume of interest (VOI)]. There are several software packages

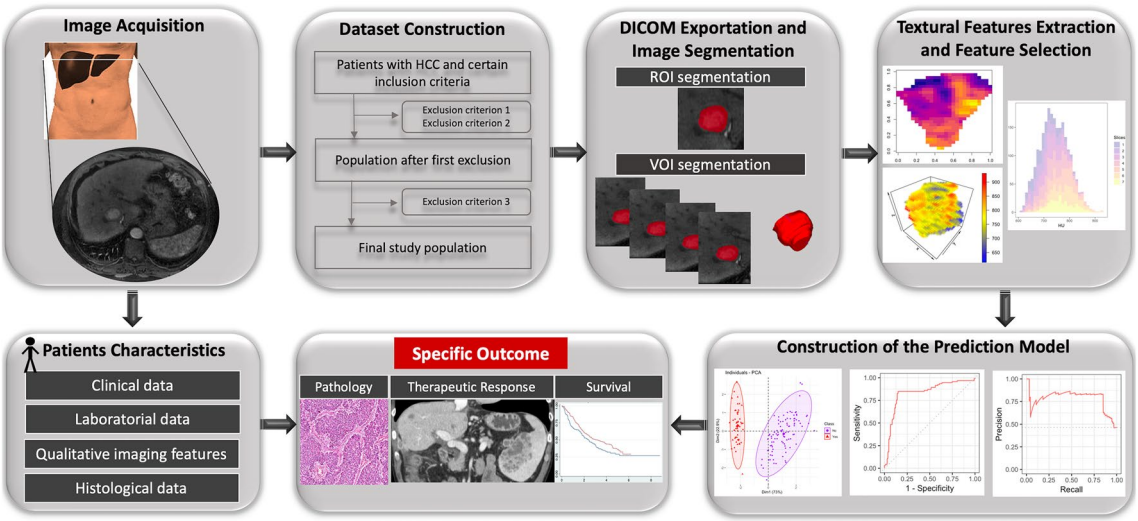


**Fig. 1** Illustration demonstrating the step-by-step radiomics process

available for imaging segmentation, some are available as a free open source tool, such as ITK-SNAP; http://itksnap.org [31]. The segmentation can be performed manually, automatically or semi-automatically;

(5) Extraction of texture features using a dedicated radiomics software;
(6) Feature selection, which identifies the most relevant features in the prediction of a given clinical endpoint;
(7) Construction of the prediction model;
(8) Validation of the model with an internal and/or external dataset [9].

## Textural features classes

A number of features can be extracted from a ROI or VOI, such as statistical-based (which evaluates the distribution of the grayscale values), model-based (evaluates the irregularity of the area), and transform-based (transforms a spatial information into frequency) methods [32]. The statistical-based model is generally the most common used.

The most common features classes are as follows:

*Morphological features* reflect volume, shape, and 3D geometric properties of the segmented ROI/VOI. Examples include diameter, surface area, volume, surface-to-volume ratio (an indirect measurement to assess spiculations), compactness, and sphericity. It also describes certain tumor characteristics, including location, vascularization, and presence of necrosis. These features are especially useful in tumor prognostication and diagnosis, including in the differentiation of benign and malignant lesions [33].

*First-order statistics features* are based on the first-order histogram that describes distribution of voxel intensities in an image. The most common first-order features are as follows: (a) *mean/median*, average intensity of the pixels in the ROI/VOI; (b) *standard deviation*, dispersion of the mean, higher values indicate a wide range of intensity of the pixels in the ROI/VOI; (c) *skewness*, asymmetry of histogram, with positive values corresponding to a longer right tail of the histogram; (d) *kurtosis*, magnitude of the histogram, with positive values indicating that the curve is taller than a normal distribution; and (e) *entropy*, irregularity or randomness of the intensities, high values demonstrate a more heterogeneous area [34] (Figs. 2, 3).

*Second-order statistics features* consider the inter-voxel relationships in an image [34]. Using grey level dependence matrices, the second-order statistical features can be classified into three groups: (a) grey level co-occurrence matrix (GLCM); (b) grey level run length matrix (GLRLM); and (c) grey level size zone matrix (GLSZM) [35]. While GLCM considers the incidence of voxels of the same grey value at a predetermined distance along a fixed direction, GLRLM considers the incidence of voxels of the more than one grey

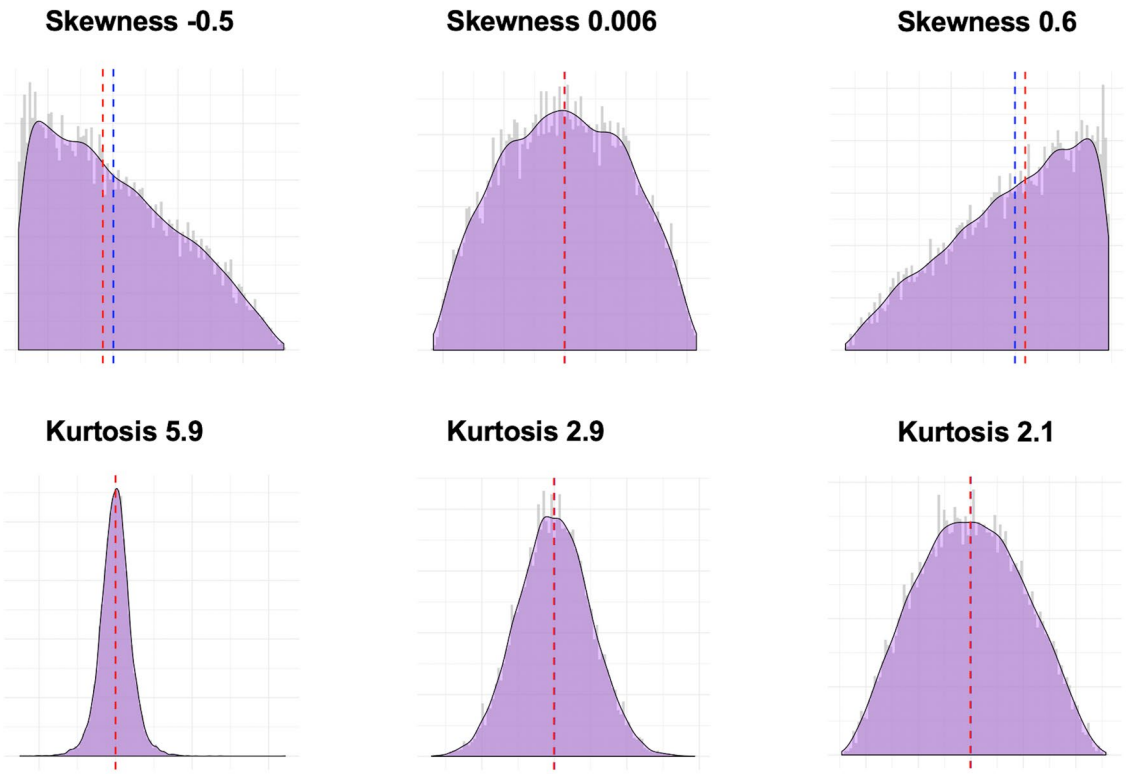


**Fig. 2** Illustration showing some first-order statistical textural features, such as skewness, kurtosis, mean (red line), and median (blue line)

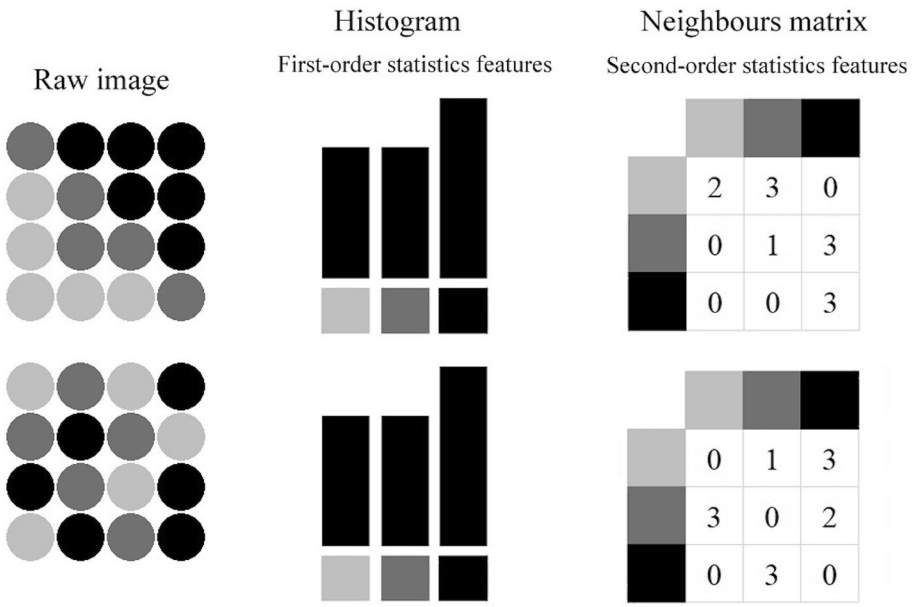


**Fig. 3** Illustration comparing first- and second-order statistics features. Note that two different images have the same number of black, light gray, gray, and dark gray pixels, producing the same histogram (first-order statistics features). On the other hand, the second-order statistics features, which took into account the horizontal direction of the pixels, resulted in different matrices. This illustration shows that first-order statistics do not take into account the interaction of the pixels, while second-order statistic features provide an information regarding the relationship between the pixels, therefore better demonstrates intra-lesion heterogeneity

value using a fixed direction and GLSZM uses all matrix directions in the same evaluation (Fig. 3).

*Superior or higher-order statistics features* these features have the advantage of considering the relationship with neighboring voxels [36] and are obtained using neighborhood grayscale difference matrices [32]. In this process, higher-order statistical methods impose filter grids on the image to extract repetitive or nonrepetitive patterns [9].

## Feature extraction software

Many research groups have developed in-house and freely available radiomics software packages to allow the advancement of radiomics research. These open-source packages are available in Matlab, Python, and R, the most popular programming tools for data science at the moment. These platforms support DICOM, NIfTI (Neuroimaging Informatics Technology Initiative) and/or nrrd (nearly raw raster data) file formats, with the feature extraction in both 2D and 3D on a ROI ("segment-based") or feature maps ("voxel-based") [37–39]. The main package documents can be found on-line (https://cran.rproject.org/web/packages/radiomics/index.html; https://cran.r-project.org/web/packages/RIA/index.html; https://pyradiomics.readthedocs.io/en/latest).

## Textural feature selection

Once the features have been extracted, a wide range of statistical tools can be used to choose a subset of features that correlate with thespecific endpoint of the study [40]. In this process, supervised or unsupervised approaches can be applied using dimensionality reduction algorithms. In the supervised approach, univariate or multivariate statistical models are often used, while cluster analysis and principal component analysis are useful strategies in the unsupervised approach. All selected features should be reproducible, nonredundant, and informative with respect to the clinical endpoint [34].

## Prediction model

Different models can be evaluated to predict a specific outcome or a response using a variety of classifiers, from simple generalized linear models to a more complex classifier, such as random forests and neural networks [31, 33]. The best models usually are those that can study a significant variety of clinical, pathologic, or genomic data, which require large high-quality data sets [9]. Of note, high-dimensional data set frequently have a far greater number of features (or variables) than the sample size study, which can lead to overfitting. Standardization methods can be used aiming to control the complexity of prediction models and to reach its appropriate capacity [31].

## Reproducibility of textural features

Some studies have evaluated the inter- and/or intra-observer agreement among radiomic features extracted from CT and MRI in patients with HCC and demonstrated high reproducibility; however, some disparities were observed in the features when extracted from patients undergoing imaging from two different scanners (Table 1) [11, 12, 17, 19, 24].

Perrin et al. [16] specifically assessed the reproducibility of liver CT features between two different scans obtained up to 2 weeks apart. The authors showed that the reproducibility of some textural features varied changing the contrast injection rate, pixel resolution and scanner model. The other

**Table 1** Summary of the studies that evaluated the reproducibility of textural features

| Author | IM | ES | Segmentation | Readers (*n*) | FE | Type | Main results | *n* (training/validation sets) |
|---|---|---|---|---|---|---|---|---|
| Perrin et al. [16] | CECT | Matlab | Semi-automatic | 2 | FO TF<br>SO TF | Reproducibility of TF between two scanners | Reproducibility of some TF varied with the changes in contrast injection rate, pixel resolution and scanner model | 38 |
| Zhou et al. [12, 13] | CECT | Matlab | Manual ROI | 2 | Morf<br>FO TF<br>SO TF | Inter- and intra-observer | Inter-observer ICC 0.75–0.90<br>Intra-observer ICC 0.80–0.9 | 215 |
| Cai et al. [17] | CECT | Python | Semi-automatic ROI | 2 | Morf<br>FO TF<br>SO TF | Inter- and intra-observer | Intra-observer ICC (liver) 0.84–0.92<br>Intra-observer ICC (tumor) 0.87–0.94<br>Inter-observer ICC (liver) 0.87–0.94<br>Inter-observer ICC (tumor) 0.88–0.94 | T: 80<br>V: 32 |
| Zheng et al. [11] | CECT | Matlab | Manual ROI | 2 | Morf<br>FO TF | Inter- and intra-observer | Inter-observer ICC 0.71–0.95<br>Intra-observer ICC 0.83–0.99 | T: 212<br>V: 107 |
| Chen et al. [19] and Feng et al. [24] | MRI (3 T) | In-house | Manual and semi-automatic VOI | 3 | Morf<br>FO TF<br>SO TF | Inter- and intra-observer | Inter-observer ICC:<br>• > 0.80: 82%<br>• 0.50–0.79: 10%<br>• < 0.50: 8%<br>Intra-observer ICC:<br>• > 0.80: 85%<br>• 0.50–0.79: 14%<br>• < 0.50: 1% | T: 150<br>V: 57 |
| Kim et al. [21] | MRI (1.5 T or 3 T) | Python | Semi-automatic VOI | 2 (30) | SO TF | Inter-observer | Inter-observer ICC: median 0.99, range 0.81–0.99 | T: 128<br>V: 39 |

*CECT* contrast-enhanced computed tomography, *ES* extraction software, *FE* feature extraction, *FO* first order, *ICC* intra-class correlation coefficient, *IM* imaging modality, *Morf* morphological, *MRI* Magnetic resonance imaging, *n* number, *ROI* region of interest, *SO* second order, *SupO* superior order, *TF* texture features, *VOI* volume of interest

studies demonstrated that the vast majority of the textural features had good and excellent inter- and intra-observer agreement, with an intra-class correlation coefficients varied from 0.71 to 0.99 [11, 12, 17, 19, 24].

## Limitations and challenges

The reproducibility of the textural features of HCC is of key importance to clinical implementation. Considering that there are several imaging protocols and equipment among different institutions and that these variations can directly affect radiomic features, efforts are needed to provide a standardized methodology to extract and process the features.

There is currently a lack of standardization on the number of texture features extracted and on the creation of prediction models, limiting the generalizability of the results. Clinical conditions, such as the presence of artifacts due to metallic prostheses, may also affect image quality and impair quantitative analysis [34, 41, 42].

Another consideration is that the number of extracted features usually is larger than the study population, which can cause overfitting of the model and overoptimistic results. Unbalanced data may require the use of oversampling techniques, which may artificially improve the performance of the model [41, 42].

Additional to these limitations, data sharing among institutions remain challenging due to legitimate concerns related to patient privacy that can limit the pathway to external validation—a crucial step in the assessment of prediction model accuracy.

# Applications of radiomics in HCC

## Pathological results

MVI is the leading independent predictor of early recurrence and, consequently, survival in patients with HCC after surgery [43–45]. MVI is diagnosed postoperatively and it is defined as the presence of tumor within portal vein, hepatic vein, or large capsular vessel [46]. Several studies have developed radiomic models to predict MVI preoperatively (Table 2). The accuracy in the prediction

**Table 2** Summary of the studies that evaluated radiomics in the preoperative prediction of microvascular invasion

| Author | IM | ES | Segmentation | Readers (*n*) | FE | M | Main results | V | *n* (training/validation sets) |
|---|---|---|---|---|---|---|---|---|---|
| Xu et al. [22] | CECT | Python | Semi-automatic VOI (AP and VP) | 2 (Consensus Li-score) 3 (radiomics) | Morf<br>FO TF | Y | Risk model (clinical, radiological and radiomics score):<br>AUC (T) 0.91<br>AUC (V) 0.89<br>Association with recurrence and mortality | I | T: 350<br>V: 145 |
| Zheng et al. [18] | CECT | Matlab | Semi-automatic ROI | 2 | Morf<br>FO TF<br>SO TF | Y | Radiomics from tumor and peritumoral regions:<br>AUC 0.80 in ≤ 5 cm tumors<br>AUC 0.75 in > 5 cm tumors<br>Multivariate model in > 5 cm tumors (radiomics, AFP, larger tumor size, and history of viral hepatitis): AUC 0.88 | N | 120 |
| Peng et al. [15] | CECT | Matlab | Semi-automatic and manual ROI (AP and VP) | 2 | Morf<br>FO TF<br>SO TF<br>SupO | Y | Nomogram (AFP, qualitative radiological features and radiomics):<br>*c*-index (T) 0.85<br>*c*-index (V) 0.84 | I | T: 184<br>V: 120 |
| Bakr et al. [23] | MRI | In-house | Manual ROI (AP, VP and DP) | 4 | Morf<br>FO TF | Y | Radiomics from tumor and peritumoral regions:<br>AUC (T) 0.85<br>AUC (V) 0.83 | N | 28 |
| Feng et al. [24] | MRI | In-house | Manual VOI | 3 | FO TF<br>SO TF | Y | Radiomics features:<br>AUC 0.76 | N | 160 |

*AFP* alpha-fetoprotein, *AP* arterial phase, *AUC* area under the curve, *CECT* contrast-enhanced computed tomography, *DP* delayed phase, *ES* extraction software, *FE* feature extraction, *FO* first order. *I* internal, *IM* imaging modality, *Li-score* structural liver imaging score based on qualitative assessment, *M* model, *Morf* morphological, *MRI* magnetic resonance imaging, *n* number, *N* no, *ROI* region of interest, *SO* second order, *SupO* superior order, *T* training, *TF* texture features, *V* validation, *VOI* volume of interest, *VP* venous phase, *Y* yes

of histological MVI varied between 0.76 and 0.91 and the models that included clinical variables obtained higher performance.

Xu et al. [22] investigated MVI prediction in contrast-enhanced CT images and found that textural features alone did not add value to radiologist scores, such as Li-score (a structural liver imaging score based on qualitative assessment), in predicting MVI. However, textural features in association with clinical and radiological qualitative biomarkers were independent predictors of MVI. This might be associated with imaging and measurement methodologies, as indicated by the authors. The model was able to identify more than 88% of MVI-positive cases with a specificity around 78%. The model was also associated with recurrence and mortality. Peng et al. [15] also did a combined prediction model in patients with hepatitis B and obtained a nomogram with *c*-index of 0.85 in the training set and 0.84 in the validation group. On the other hand, Feng et al. [24] using only textural features obtained an area under the curve (AUC) of 0.76.

Considering that MVI commonly occurs in the tumor edges, some authors also extracted the features from the peritumoral area. Xu et al. [22] found that these features obtained on CT were different among patients with and without MVI; however, the accuracy was not higher than the one obtained from the tumor area. In contrast, Bakr et al. [23] developed a combined model using both tumoral and peritumoral textural features on MRI and obtained higher performance with an accuracy of 0.83. Zheng et al. [18] also showed that quantitative image analysis of tumoral and peritumoral can predict MVI and that the addition of clinical data improved the predictive model among larger tumors.

## Treatment selection or outcome

Several studies evaluated the performance of radiomics in predicting survival and recurrence after hepatectomy, which is one of the potential curative treatments for HCC, particularly for patients with large lesions and preserved liver function. The number of patients in these studies varied from 50 to 495 and included CT and MRI. The AUC varied between 0.59 and 0.91 [11, 12, 21, 22, 25–28]. Table 3 summarizes these studies.

Zhou et al. [12] found that incorporating the radiomics signature based on CT texture features into conventional preoperative variables significantly improved the accuracy of the clinical model in predicting early recurrence when compared to those conventional variables alone (AUC of the combined model was 0.84). The conventional variables used in this study were age, alpha-fetoprotein, aspartate aminotransferase, gama glutamyltranspeptidase, tumor size, liver segment involved, contact with liver capsule, Barcelona Clinic Liver Cancer (BCLC) stage, and radiological evidence of internal arteries, necrosis, or vascular invasion [12]. Similar results were documented by other groups. Xu et al. [22] found that a risk model integrating clinicoradiological factors and radiomic-scores was independently associated with disease-specific recurrence and long-term mortality. The following variables were used: aspartate aminotransferase > 40 U/L, alpha-fetoprotein > 400, nonsmooth tumor margin, extrahepatic growth pattern, ill-defined pseudo-capsule, peritumoral arterial enhancement, and high radiomic score.

Kim et al. [21] included the peritumoral (border extension of 3 mm) in preoperative radiomic model using gadoxetic acid-enhanced MRI and demonstrated a comparable performance to that of the postoperative clinicopathologic model for predicting early recurrence. Shan et al. [28] also delineated the tumor and the peritumoral area. The model based on tumoral features demonstrated an AUC of 0.82 in the training set and 0.62 in the validation set, while the one based on peritumoral area obtained an AUC of 0.80 in the training set and 0.79 in the validation cohort. These results suggest that radiomic features extracted from peritumoral region may also provide relevant information.

## Prognosis

Surgical resection and liver transplantation are not always feasible for a majority of the patients with HCC [47–49]. In this scenario, locoregional therapies have gained increased acceptance as a therapeutic option, and include modalities such as radiofrequency ablation, transarterial chemoembolization (TACE), and transarterial radioembolization (TARE).

Few studies have evaluated texture-based features to predict survival, including overall survival and progression-free survival and treatment response after locoregional therapies (Table 3).

Regarding survival after locoregional treatment, Shan et al. [28] included CT from patients after hepatectomy and radiofrequency ablation. The AUC in predicting recurrence varied from 0.62 to 0.82, being higher using peritumoral radiomic features than the tumoral radiomic model or peritumoral enhancement. A study also evaluated CT in predicting survival in patients after TACE [20]. They demonstrated that a combined score model that integrated radiomic features with clinical data (Child–Pugh score, alpha-fetoprotein, and HCC size) better predicted survival. Finally, Blanc-Durand et al. [50] have evaluated 18-fluoro-deoxyglucose positron emission tomography (FDG-PET) before TARE and the whole-liver radiomics textural features were an independent negative predictor for survival. Furthermore, radiomic scoring system did not differ after stratification by BCLC staging and tumor size.

With regards to treatment response, one study has evaluated radiomic features on CT. Park et al. [51] revealed that HCC with complete response after TACE exhibited on pretreatment CT significantly different values of some textural features when compared with patients without complete response.

## Other applications of radiomics in HCC

Wu et al. [14] reported a study that used texture analysis to discriminate the grade of HCC based on dynamic contrast-enhanced magnetic resonance images (DCE-MR images). The authors found that low-grade HCCs showed an increase in mean intensity and a decrease in gray-level nonuniformity (GLN) in four directions (the AUC values of the average intensity and GLN in four directions were 0.92, 0.85, 0.84, 0.83, and 0.84, respectively).

Cai et al. [17] developed a CT-based radiomic model for the preoperative prediction of post-hepatectomy liver failure in patients with HCC and built a prediction model with an AUC of 0.82 in the training group and 0.76 in the validation group. The combination of radiomic signature, Model for End-Stage Liver Disease (MELD) score and Eastern Cooperative Oncology Group (ECOG) performance status increased the AUC to 0.86 in the training set and 0.90 in the validation set.

Immunotherapy using immune checkpoint blockade is a recent advance for the treatment of HCC. However, the efficacy of immunotherapy varies greatly among patients with a response rate around 20% [52, 53]. Thus, identification of potential responders to immunotherapy is critical. Previous studies showed that response and survival were closely related to the density of tumor infiltrating lymphocytes. Chen et al. [19] developed a radiomics model based on contrast-enhanced MRI for pretreatment prediction of

**Table 3** Summary of studies that evaluated radiomics in predicting recurrence and survival

| Author | Aim | Tx | IM | ES | Segmentation | Readers | FE | M | FU and recurrence criteria | Main results | V | *n* (training/validation sets) |
|---|---|---|---|---|---|---|---|---|---|---|---|---|
| Kiryu et al. [25] | Predict survival (OS and DFS) | H | NECT | TexRAD | Manual ROI | 1 | FO TF | Y | NA | Some radiomics features correlates with survival | N | 122 |
| Akai et al. [26] | Predict survival (OS and DFS) | H | CECT | TexRAD | Manual ROI | 1 | FO TF | Y | 5 years<br>Recurrence: imaging findings (2 IM) | RSF was able to stratify two risk groups<br>RSF classifier and vascular invasion were associated with OS | N | 127 |
| Hui et al. [27] | Predict early recurrence | H | MRI (1.5 T) | Matlab | Manual ROI | 3 (2 If discordance) | Morf<br>FO TF<br>SO TF<br>SupO | Y | At least 2 years<br>Recurrence: imaging findings | Some TF predicted recurrence<br>AUC 0.78–0.84 | N | 50 |
| Zhou et al. [12, 13] | Predict early recurrence | H | CECT | Matlab | Manual ROI | 2 (Consensus) | Morf<br>FO TF<br>SO TF | Y | 1 year<br>Recurrence: typical imaging findings, biopsy-proven, new lesions or metastases | Radiomics model:<br>*S* 0.79<br>Sp 0.70<br>AUC 0.82<br>Combined model:<br>*S* 0.82<br>Sp 0.71<br>AUC 0.84 | N | 215 |
| Xu et al. [22] | Predict MVI and survival | H or LT | CECT | Python | Semi-automatic VOI | 3 | Morf<br>FO TF | Y | NA | AUC of the risk model:<br>T: 0.91/V: 0.89<br>Clinical, qualitative and TF | I | T: 350<br>V: 145 |
| Guo et al. [30] | Predict recurrence | LT | CECT | Python | Semi-automatic VOI | 1 (15 Exams were re-segmented by another radiologist) | Morf<br>FO TF | Y | 5 years<br>Recurrence: imaging findings (2 IM) | Radiomics model:<br>AUC (T) 0.74<br>AUC (V) 0.71<br>Combined model:<br>AUC (T) 0.79<br>AUC (V) 0.79 | I | T: 93<br>V: 40 |
| Zheng et al. [11] | Predict recurrence and survival | H | CECT | Matlab | Manual ROI | 2 | Morf<br>FO TF | Y | NA | Recurrence AUC (T) 0.64<br>Recurrence AUC (V) 0.59<br>Survival AUC (T) 0.71<br>Survival AUC (V) 0.71 | I | T: 212<br>V: 107 |
| Kim et al. [21] | Predict recurrence | H | MRI (1.5 T or 3 T) | Python | Semi-automatic VOI | 1 (30 Exams were re-segmented by another radiologist) | SO TF | Y | At least 2 years<br>Recurrence: imaging findings | Clinicopathologic-radiomic model was able to stratify two risk groups<br>*c*-index 0.716<br>Tumoral and peritumoral | I | T: 128<br>V: 39 |

**Table 3** (continued)

| Author | Aim | Tx | IM | ES | Segmentation | Readers | FE | M | FU and recurrence criteria | Main results | V | *n* (training/validation sets) |
|---|---|---|---|---|---|---|---|---|---|---|---|---|
| Shan et al. [28] | Predict recurrence | H or A | CECT | In-house | Manual ROI | 2 (Consensus) | FO TF | Y | Recurrence: new typical hepatic lesions or metastases on IM or biopsy-proven lesions | Peritumoral TF:<br>AUC (T) 0.80<br>AUC (V) 0.79 | I | T: 109<br>V: 47 |
| Kim et al. [20] | Predict survival (OS and PFS) | TACE | CECT | Matlab | Manual ROI | 1 | Morf<br>FO TF<br>SO TF | Y | NA | Combining clinical and radiomic features better predicted survival | N | NA |
| Blanc-Durand et al. [50] | Predict survival (OS and PFS) | $^{90}$Y-TARE | $^{18}$F-FDG PET–CT | MITK | Semi-automatic VOI | NA | Morf<br>FO TF<br>SO TF | Y | Recurrence: imaging findings | Whole-liver TF were independent negative predictor for PFS and OS | N | NA |

*A* ablation, *AFP*alpha-fetoprotein, *AST* aspartate aminotransferase, *AUC* area under the curve, *CECT* contrast-enhanced computed tomography, *ES* extraction software, *FE* feature extraction, *FO* first order, *FU* follow-up, *H* hepatectomy, *I* internal, *IM* imaging modality, *LT* liver transplantation, *M* model, *mo* months, *Morf* morphological, *MRI* magnetic resonance imaging, *N* no, *NECT* noncontrast-enhanced computed tomography, *NA* not available, *OS* overall survival, *PET* positron emission tomography, *PFS* progression-free survival, *ROI* region of interest, *RSF* random survival forest, *S* sensitivity, *Segm* segmentation, *SO* second order, *Sp* specificity, *SupO* superior order, *T* training, *TACE* transarterial chemoembolization, *$^{90}$Y-TARE* transarterial radioembolization using yttrium-90, *TF* texture features, *Tx* treatment, *V* validation, *VMAT* volumetric modulated arc therapy, *VOI* volume of interest, *Y* yes

immunoscore in HCC, and found that incorporating peritumoral radiomic analysis improved the estimation of immunoscore of tumor infiltrating lymphocytes.

## Conclusion

Radiomics is a rapidly evolving computer-assisted tool with the potential to improve the management of HCC patients, allowing the application of a personalized medicine to patients with HCC, avoiding unnecessary procedures, reducing the cost and optimizing the available resources. The studies described here demonstrated for the most part that textural features alone could predict pathological results, such as MVI and histological grade, guide treatment selection, predict patient outcome and prognosis. In addition, when combined to clinical data models better prediction models were observed.

Up to now, some studies have evaluated the use of radiomics in HCC with promising results. However, there are challenges to be overcome before its implementation into clinical practice. Some specific issues need to be considered before its wide implementation, particularly related to the numerous methodological variability, uncertain reproducibility, the need of standardization of imaging acquisition, and the lack of robust validation with multicenter patient populations. Another important concern is the imaging segmentation that is a time-consuming step. In this context, automatic and semi-automatic segmentation tools have the potential to optimize this process and, eventually, increase its acceptance in clinical practice.

In conclusion, it is important to radiologists to be aware of the basic principles, benefits, and limitations of radiomics in HCC in order to translate these promising results towards clinical care. Further studies are important to improvethe accuracy of radiomic models, especially prospective and multicenter ones.

**Acknowledgements** The authors would like to express their deepest gratitude to Dr. Richard Kinh Gian Do, MD, PhD radiologist at Memorial Sloan Kettering Cancer Center for his support on this manuscript.

**Funding** No funding was received.

### Compliance with ethical standards

**Conflict of interest** The authors declare that they have no conflict of interest.

## References

1. Ferlay J, Soerjomataram I, Dikshit R, Eser S, Mathers C, Rebelo M, et al. Cancer incidence and mortality worldwide: sources, methods and major patterns in GLOBOCAN 2012. Int J Cancer. 2015;136(5):E359-86.
2. Torre LA, Bray F, Siegel RL, Ferlay J, Lortet-Tieulent J, Jemal A. Global cancer statistics, 2012. CA Cancer J Clin. 2015;65(2):87-108.
3. Llovet JM, Bustamante J, Castells A, Vilana R, Ayuso MeC, Sala M, et al. Natural history of untreated nonsurgical hepatocellular carcinoma: rationale for the design and evaluation of therapeutic trials. Hepatology. 1999;29(1):62-7.
4. Mittal S, El-Serag HB. Epidemiology of hepatocellular carcinoma: consider the population. J Clin Gastroenterol. 2013;47 Suppl:S2-6.
5. Venook AP, Papandreou C, Furuse J, de Guevara LL. The incidence and epidemiology of hepatocellular carcinoma: a global and regional perspective. Oncologist. 2010;15 Suppl 4:5-13.
6. Cruite I, Tang A, Sirlin CB. Imaging-based diagnostic systems for hepatocellular carcinoma. AJR Am J Roentgenol. 2013;201(1):41-55.
7. Horvat N, Monti S, Oliveira BC, Rocha CCT, Giancipoli RG, Mannelli L. State of the art in magnetic resonance imaging of hepatocellular carcinoma. Radiol Oncol. 2018;52(4):353-64.
8. Horvat N, Nikolovski I, Long N, Gerst S, Zheng J, Pak LM, et al. Imaging features of hepatocellular carcinoma compared to intrahepatic cholangiocarcinoma and combined tumor on MRI using liver imaging and data system (LI-RADS) version 2014. Abdom Radiol (NY). 2018;43(1):169-78.
9. Gillies RJ, Kinahan PE, Hricak H. Radiomics: Images Are More than Pictures, They Are Data. Radiology. 2016;278(2):563-77.
10. Horvat N, Bates DDB, Petkovska I. Novel imaging techniques of rectal cancer: what do radiomics and radiogenomics have to offer? A literature review. Abdom Radiol (NY). 2019.
11. Zheng BH, Liu LZ, Zhang ZZ, Shi JY, Dong LQ, Tian LY, et al. Radiomics score: apotential prognostic imaging feature for postoperative survival of solitary HCC patients. BMC Cancer. 2018;18(1):1148.
12. Zhou Y, He L, Huang Y, Chen S, Wu P, Ye W, et al. CT-based radiomics signature: a potential biomarker for preoperative prediction of early recurrence in hepatocellular carcinoma. Abdom Radiol (NY). 2017;42(6):1695-704.
13. Zhou W, Zhang L, Wang K, Chen S, Wang G, Liu Z, et al. Malignancy characterization of hepatocellular carcinomas based on texture analysis of contrast-enhanced MR images. J Magn Reson Imaging. 2017;45(5):1476-84.
14. Wu M, Tan H, Gao F, Hai J, Ning P, Chen J, et al. Predicting the grade of hepatocellular carcinoma based on non-contrast-enhanced MRI radiomics signature. Eur Radiol. 2018.
15. Peng J, Zhang J, Zhang Q, Xu Y, Zhou J, Liu L. A radiomics nomogram for preoperative prediction of microvascular invasion risk in hepatitis B virus-related hepatocellular carcinoma. Diagn Interv Radiol. 2018;24(3):121-7.
16. Perrin T, Midya A, Yamashita R, Chakraborty J, Saidon T, Jarnagin WR, et al. Short-term reproducibility of radiomic features in liver parenchyma and liver malignancies on contrast-enhanced CT imaging. Abdom Radiol (NY). 2018;43(12):3271-8.
17. Cai W, He B, Hu M, Zhang W, Xiao D, Yu H, et al. A radiomics-based nomogram for the preoperative prediction of posthepatectomy liver failure in patients with hepatocellular carcinoma. Surg Oncol. 2019;28:78-85.
18. Zheng J, Chakraborty J, Chapman WC, Gerst S, Gonen M, Pak LM, et al. Preoperative Prediction of Microvascular Invasion in Hepatocellular Carcinoma Using Quantitative Image Analysis. J Am Coll Surg. 2017;225(6):778-88.e1.
19. Chen S, Feng S, Wei J, Liu F, Li B, Li X, et al. Pretreatment prediction of immunoscore in hepatocellular cancer: a radiomics-based clinical model based on Gd-EOB-DTPA-enhanced MRI imaging. Eur Radiol. 2019.

20. Kim J, Choi SJ, Lee SH, Lee HY, Park H. Predicting Survival Using Pretreatment CT for Patients With Hepatocellular Carcinoma Treated With Transarterial Chemoembolization: Comparison of Models Using Radiomics. AJR Am J Roentgenol. 2018;211(5):1026-34.
21. Kim S, Shin J, Kim DY, Choi GH, Kim MJ, Choi JY. Radiomics on Gadoxetic Acid-Enhanced Magnetic Resonance Imaging for Prediction of Postoperative Early and Late Recurrence of Single Hepatocellular Carcinoma. Clin Cancer Res. 2019.
22. Xu X, Zhang HL, Liu QP, Sun SW, Zhang J, Zhu FP, et al. Radiomic analysis of contrast-enhanced CT predicts microvascular invasion and outcome in hepatocellular carcinoma. J Hepatol. 2019.
23. Bakr S, Echegaray S, Shah R, Kamaya A, Louie J, Napel S, et al. Noninvasive radiomics signature based on quantitative analysis of computed tomography images as a surrogate for microvascular invasion in hepatocellular carcinoma: a pilot study. J Med Imaging (Bellingham). 2017;4(4):041303.
24. Feng ST, Jia Y, Liao B, Huang B, Zhou Q, Li X, et al. Preoperative prediction of microvascular invasion in hepatocellular cancer: a radiomics model using Gd-EOB-DTPA-enhanced MRI. Eur Radiol. 2019.
25. Kiryu S, Akai H, Nojima M, Hasegawa K, Shinkawa H, Kokudo N, et al. Impact of hepatocellular carcinoma heterogeneity on computed tomography as a prognostic indicator. Sci Rep. 2017;7(1):12689.
26. Akai H, Yasaka K, Kunimatsu A, Nojima M, Kokudo T, Kokudo N, et al. Predicting prognosis of resected hepatocellular carcinoma by radiomics analysis with random survival forest. Diagn Interv Imaging. 2018;99(10):643-51.
27. Hui TCH, Chuah TK, Low HM, Tan CH. Predicting early recurrence of hepatocellular carcinoma with texture analysis of preoperative MRI: a radiomics study. Clin Radiol. 2018;73(12):1056.e11-.e16.
28. Shan QY, Hu HT, Feng ST, Peng ZP, Chen SL, Zhou Q, et al. CT-based peritumoral radiomics signatures to predict early recurrence in hepatocellular carcinoma after curative tumor resection or ablation. Cancer Imaging. 2019;19(1):11.
29. Wu J, Liu A, Cui J, Chen A, Song Q, Xie L. Radiomics-based classification of hepatocellular carcinoma and hepatic haemangioma on precontrast magnetic resonance images. BMC Med Imaging. 2019;19(1):23.
30. Guo D, Gu D, Wang H, Wei J, Wang Z, Hao X, et al. Radiomics analysis enables recurrence prediction for hepatocellular carcinoma after liver transplantation. Eur J Radiol. 2019;117:33-40.
31. Larue RT, Defraene G, De Ruysscher D, Lambin P, van Elmpt W. Quantitative radiomics studies for tissue characterization: a review of technology and methodological procedures. Br J Radiol. 2017;90(1070):20160665.
32. Lubner MG, Smith AD, Sandrasegaran K, Sahani DV, Pickhardt PJ. CT Texture Analysis: Definitions, Applications, Biologic Correlates, and Challenges. Radiographics: a review publication of the Radiological Society of North America, Inc. 2017;37(5):1483-503.
33. Thawani R, McLane M, Beig N, Ghose S, Prasanna P, Velcheti V, et al. Radiomics and radiogenomics in lung cancer: A review for the clinician. Lung cancer (Amsterdam, Netherlands). 2018;115:34-41.
34. Rizzo S, Botta F, Raimondi S, Origgi D, Fanciullo C, Morganti AG, et al. Radiomics: the facts and the challenges of image analysis. Eur Radiol Exp.2018;2(1):36.
35. Horvat N, Bates DDB, Petkovska IJAR. Novel imaging techniques of rectal cancer: what do radiomics and radiogenomics have to offer? A literature review. 2019.
36. Bashir U, Siddique MM, McLean E, Goh V, Cook GJ. Imaging Heterogeneity in Lung Cancer: Techniques, Applications, and Challenges. AJR American journal of roentgenology. 2016;207(3):534-43.
37. Kolossváry M, Karády J, Szilveszter B, Kitslaar P, Hoffmann U, Merkely B, et al. Radiomic Features Are Superior to Conventional Quantitative Computed Tomographic Metrics to Identify Coronary Plaques With Napkin-Ring Sign. Circ Cardiovasc Imaging. 2017;10(12).
38. Parmar C, Grossmann P, Bussink J, Lambin P, Aerts HJ. Machine Learning methods for Quantitative Radiomic Biomarkers. Sci Rep. 2015;5:13087.
39. van Griethuysen JJM, Fedorov A, Parmar C, Hosny A, Aucoin N, Narayan V, et al. Computational Radiomics System to Decode the Radiographic Phenotype. Cancer Res. 2017;77(21):e104-e7.
40. Parmar C, Grossmann P, Bussink J, Lambin P, Aerts H. Machine Learning methods for Quantitative Radiomic Biomarkers. Scientific reports. 2015;5:13087.
41. Chawla NV, Bowyer KW, Hall LO, Kegelmeyer WP. SMOTE: Synthetic minority over-sampling technique. J Artif Intell Res. 2002;16:321-57.
42. Fehr D, Veeraraghavan H, Wibmer A, Gondo T, Matsumoto K, Vargas HA, et al. Automatic classification of prostate cancer Gleason scores from multiparametric magnetic resonance images. Proc Natl Acad Sci U S A. 2015;112(46):E6265-73.
43. Lim KC, Chow PK, Allen JC, Chia GS, Lim M, Cheow PC, et al. Microvascular invasion is a better predictor of tumor recurrence and overall survival following surgical resection for hepatocellular carcinoma compared to the Milan criteria. Ann Surg. 2011;254(1):108-13.
44. Mazzaferro V, Llovet JM, Miceli R, Bhoori S, Schiavo M, Mariani L, et al. Predicting survival after liver transplantation in patients with hepatocellular carcinoma beyond the Milan criteria: a retrospective, exploratory analysis. Lancet Oncol. 2009;10(1):35-43.
45. Imamura H, Matsuyama Y, Tanaka E, Ohkubo T, Hasegawa K, Miyagawa S, et al. Risk factors contributing to early and late phase intrahepaticrecurrence of hepatocellular carcinoma after hepatectomy. J Hepatol. 2003;38(2):200-7.
46. Rodríguez-Perálvarez M, Luong TV, Andreana L, Meyer T, Dhillon AP, Burroughs AK. A systematic review of microvascular invasion in hepatocellular carcinoma: diagnostic and prognostic variability. Ann Surg Oncol. 2013;20(1):325-39.
47. Torzilli G, Makuuchi M, Inoue K, Takayama T, Sakamoto Y, Sugawara Y, et al. No-mortality liver resection for hepatocellular carcinoma in cirrhotic and noncirrhotic patients: is there a way? A prospective analysis of our approach. Arch Surg. 1999;134(9):984-92.
48. Fan ST, Lo CM, Liu CL, Lam CM, Yuen WK, Yeung C, et al. Hepatectomy for hepatocellular carcinoma: toward zero hospital deaths. Ann Surg. 1999;229(3):322-30.
49. Hasegawa K, Kokudo N, Imamura H, Matsuyama Y, Aoki T, Minagawa M, et al. Prognostic impact of anatomic resection for hepatocellular carcinoma. Ann Surg. 2005;242(2):252-9.
50. Blanc-Durand P, Van Der Gucht A, Jreige M, Nicod-Lalonde M, Silva-Monteiro M, Prior JO, et al. Signature of survival: a. Oncotarget. 2018;9(4):4549-58.
51. Park HJ, Kim JH, Choi SY, Lee ES, Park SJ, Byun JY, et al. Prediction of Therapeutic Response of Hepatocellular Carcinoma to Transcatheter Arterial Chemoembolization Based on

Pretherapeutic Dynamic CT and Textural Findings. AJR Am J Roentgenol. 2017;209(4):W211-W20.
52. El-Khoueiry AB, Sangro B, Yau T, Crocenzi TS, Kudo M, Hsu C, et al. Nivolumab in patients with advanced hepatocellular carcinoma (CheckMate 040): an open-label, non-comparative, phase 1/2 dose escalation and expansion trial. Lancet. 2017;389(10088):2492-502.
53. Sangro B, Gomez-Martin C, de la Mata M, Iñarrairaegui M, Garralda E, Barrera P, et al. A clinical trial of CTLA-4 blockade with tremelimumab in patients with hepatocellular carcinoma and chronic hepatitis C. J Hepatol. 2013;59(1):81-8.